Related topics

Bohr's atomic model, quantisation of energy levels, electron spin, Bohr's magneton, interference of electromagnetic waves, Fabry-Perot interferometer.

Principle

The "Zeeman effect" is the splitting up of the spectral lines of atoms within a magnetic field. The simplest is the splitting up of one spectral line into three components called the "normal Zeeman effect". The normal Zeeman effect is studied using a cadmium spectral lamp as a specimen. The cadmium lamp is submitted to different magnetic flux densities and the splitting up of the red cadmium line (643.8 nm) is investigated using a Fabry-Perot interferometer. The evaluation of the results leads to a fairly precise value for Bohr's magneton.

Material

1	Fabry-Perot interferometer	09050-02
1	Cadmium lamp for Zeeman effect	09050-20
1	Electromagnet w/o pole shoes	06480-01
1	Pole pieces, drilled, conical	06480-03
1	Rot.table for heavy loads	02077-00
1	Power supply for spectral lamps	13662-97
1	Variable transformer, 25 VAC/ 20 VDC, 12 A	13531-93
1	Capacitor,electrolyt.,22000 µF	06211-00
1	DMM with NiCr-Ni thermo couple	07122-00
1	Optical profile-bench, l 1000mm	08282-00
2	Base for optical bench, adjustable	08284-00
5	Slide mount for optical bench, h = 30 mm	08286-01
2	Slide mount for optical bench, h = 80 mm	08286-02
4	Lens holder	08012-00
2	Lens, mounted, f +50 mm	08020-01
1	Lens, mounted, f +300 mm	08023-01
1	Iris diaphragm	08045-00
1	Polarising filter,on stem	08610-00
1	Polarization specimen, mica	08664-00
1	Connecting cord, 32 A, 250 mm, red	07360-01
1	Connecting cord, 32 A, 250 mm, blue	07360-04
1	Connecting cord, 32 A, 500 mm, red	07361-01
1	Connecting cord, 32 A, 500 mm, blue	07361-04
1	Connecting cord, 32 A, 750 mm, red	07362-01
1	Connecting cord, 32 A, 1000 mm, red	07363-01
1	Connecting cord, 32 A, 1000 mm, blue	07363-04
1	Sliding device, horizontal	08713-00
1	Plate holder with tension spring	08288-00
1	Screen, with aperture and scale	08340-00
1	Swinging arm	08256-00

Fig. 1: Experimental setup.

Tasks

1. Using the Fabry-Perot interferometer, a self-made telescope, a sliding device and a screen with scale, the splitting up of the central line into two σ-lines is measured in wave numbers as a function of the magnetic flux density. From the results of point 1. a value for Bohr's magneton is evaluated.
2. The light emitted within the direction of the magnetic field is qualitatively investigated.

Set-up and procedure

The electromagnet is put on the rotating table for heavy loads and mounted with the two pole-shoes with holes in such a way that a gap large enough for the Cd-lamp (9-11 mm) remains for the Cd-lamp. The pole-shoes have to be well tightened in such a way that they cannot move later on when the magnetic flux is established. The Cd-lamp is inserted into the gap without touching the pole-shoes and connected to the power supply for spectral lamps. The coils of the electromagnet are connected in parallel and via an ammeter connected to the variable power supply of up to 20 VDC, 12 A. A capacitor of 22000 µF is in parallel to the power output to smoothen the DC-voltage. The optical bench for investigation of the line splitting carries the following elements (their approximate position in cm is given in brackets):

(73) L3 = +50 mm
(68) Screen with scale
(45) Analyser
(39) L2 = +300 mm
(33) Fabry-Perot Etalon
(25) L1 = +50 mm
(20) Iris diaphragm
(20) Drilled pole-shoes
(0) Cd-spectral lamp on rotating table

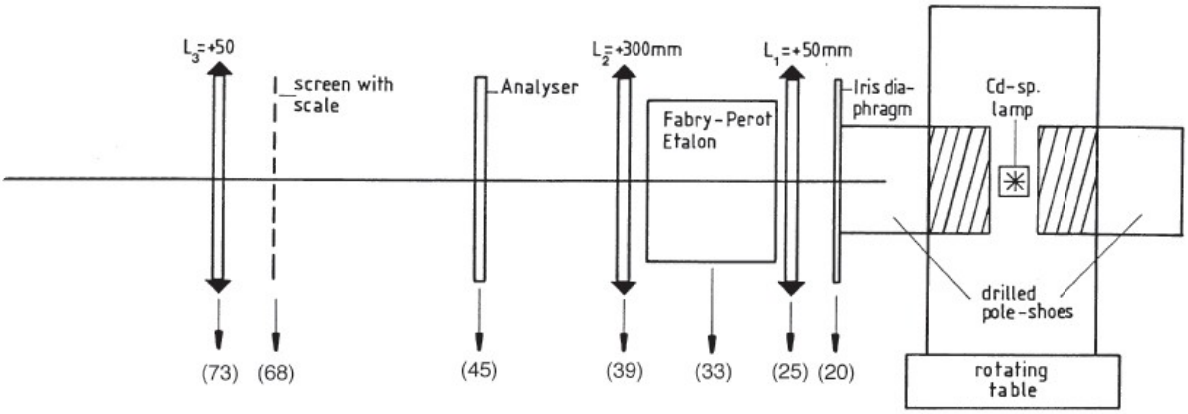

Fig. 2: Arrangement of the optical components.

The iris diaphragm is eliminated for initial adjustment and for the observation of the longitudinal Zeeman effect. During observation of the transverse Zeeman effect the iris diaphragm is illuminated by the Cd-lamp and such it acts as the light source. The lens L_1 and a lens of f = 100 mm, incorporated in the etalon, create a nearly parallel light beam which the Fabry-Perot etalon needs for a proper interference pattern. The etalon contains a removable colour filter that lets the red cadmium line at 643.8 nm pass. The lens L_2 produces an interference pattern of rings which can be observed through L_3. In the classical version the interference pattern is produced within the plane of the screen with a scale mounted on a slide

mount which can latterally be displaced with a precision of 1/100th of a millimeter. The measurement here can be done for instance, by systematic displacement of the slash representing the „0“ of the scale.
The initial adjustment is done in the following way:
The rotating table with electromagnet, pole-shoes and Cd-lamp already mounted is adjusted so that the center of the holes in the pole-shoes lies about 28 cm above the table. The optical bench with all elements (except iris diaphragm) mounted, is then moved closer to the electromagnet in such a way that one of the outlet holes of the poleshoes coincides with the previous position of the iris diaphragm. L_1 is then adjusted so that the outlet hole is within the focal plane of it. All other optical elements of Fig. 2. are subsequently readjusted with respect to their height correspondingly. The current of the coils is set for some time to 8 A (increase in light intensity of the Cd-lamp !) and the ring interference pattern in axial direction is observed through L_3 by the eye. The pattern must be centered and sharp which is eventually achieved by a last, slight movement of the etalon (to the right or to the left) and by displacement of L_2 (vertically and horizontally).
Hint: best results are achieved when the experiment is carried out in a darkened room.
The electromagnet is now turned by 90°, the iris diaphragm is inserted and the analyzer turned until the π-line (explanation follows) disappears completely and the two s-lines appear clearly visible.

Remark:
For later evaluations the calibration curve of the magnetic flux density versus the coil current has to be traced previously. This can be done if a teslameter is available. Otherwise the results of Fig. 3 must be used. The curve of Fig. 3 was traced by measuring the flux density in the center of the gap in the absence of the Cd-lamp. For the evaluations these center-values were increased by 3.5% to account for the non-uniform flux distribution within the gap.

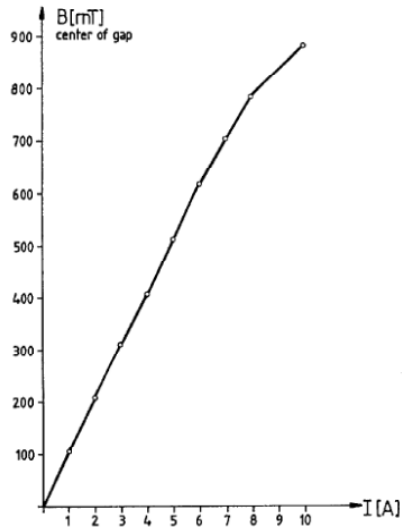

Fig. 3: Magnetic flux density B in the centre of the gap without Cd-lamp (gap width: 9 mm) as a function of the coil current.

Theory
As early as 1862, Faraday investigated whether the spectrum of coloured flames changes under the influence of a magnetic field, but without success. It was not until 1885 that Fievez from Belgium was able to demonstrate an effect, but it was forgotten and only rediscovered 11 years later by the Dutchman Zeeman, who studied it together with Lorentz.
Here the effect is demonstrated with the light of a Cadmium lamp and the help of a Fabry-Perot interferometer for resolving a small part of the spectrum preselected by a color filter or an interference filter so only the light of a single atomic transition line is observed. Without field the magnetic sub-levels have the same energy but with field the degeneration of the levels with different m_J is cancelled and the line is split. Cadmium has the electron structure (Kr) $4d^{10}\ 5s^2$, i.e. the outer shell taking part in optical transitions is composed by the two $5s^2$ electrons that represent a completed electron shell. ((Kr) = $1s^2\ 2s^2\ 2p^6\ 3s^2\ 3p^6\ 3d^{10}\ 4s^2\ 4p^6$.) This is similar to the outer electron structure of Helium but also of Mercury. A scheme of the energy levels of Cd is shown in Fig.4. In a completed shell in it's ground state the electron spins always compensate each other – they are anti-parallel. If the total electron spin is zero, also the magnetic moment connected to electron spin is zero. Atomic states with zero total spin are called singulett states. So in transitions between different singulett states the magnetic moment of spin does not play a role, as is the case with the normal Zeeman effect. Electric dipole radiation as in common optical transitions does not change the electron spin except in heavy atoms with *jj*-coupling, so transitions are normally between different states in the same multiplicity system. But Fig. 4 shows there is some *jj*-coupling in Cadmium.

The transition used to demonstrate the normal Zeeman effect is 3 $^1D_2 \rightarrow 2\ ^1P_1$ with 643.847 nm and the transition used to demonstrate the anomalous Zeeman effect is 2 $^3S_1 \rightarrow 2\ ^3P_2$ with 508.588 nm.
In a term like 2 $^3S_1$ the first number "2" denotes the main quantum number of the radiating electron with respect to the atom's ground state (that is counted as "1"), here this is really the 6th s-shell since $5s^2$ is the ground state. (This is why the 2 P – states are below the 2 S – states, 2 $^3P_2$ denotes the 5th p-shell since Krypton has $4p^6$.) The upper "3" denotes the multiplicity, that is 2s+1 with *s* here the spin quantum number. The lower "1" denotes the quantum number *j* of the total angular momentum, i.e.
j = l+s, l+s-1, … , l-s with *l* the quantum number of the angular momentum of the orbit. "S", "P", "D", "F" denote the actual value of *l,* i.e. "S" means *l* = 0, "P" means *l* = 1, …
3 $^1D_2 \rightarrow 2\ ^1P_1$ is a transition within the singulett system so the spin magnetic moments have no effect. But in the transition 2 $^3S_1 \rightarrow 2\ ^3P_2$ triplett states are involved and the spin magnetic moment does not vanish in all sub-states.
The selection rule for optical transitions is $\Delta m_J = 0, \pm 1$ and the radiation belonging to transitions with $\Delta m_J = 0$ are called *π*-lines and the ones with $\Delta m_J = \pm 1$ are called *σ*-lines. With the magnetic field turned on in the absence of the analyser three lines can be seen simultaneously in the normal Zeeman effect in transversal observation. In the case of the anomalous Zeeman effect three groups of three lines appear. Inserting the analyser in the normal Zeeman effect two *σ*-lines can be observed if the analyser is in the vertical position, while only the *π*-line appears if the analyser is turned into its horizontal position (transversal Zeeman effect). In the anomalous Zeeman effect there are two groups of three *σ*-lines in vertical polarization and one group of three *π*-lines in horizontal polarization. Turning the electromagnet by 90° the light coming from the spectral lamp parallel to the direction of the field (longitudinal) can also be studied trough the holes in the polepieces. It can be shown that this light is circular polarized light (longitudinal Zeeman effect). Fig. 5 summarizes the facts. A *λ*/4-plate is generally used to convert linear into elliptical polarized light. In this experiment the *λ*/4-plate is used in the opposite way. With the *λ*/4-plate inserted before the analyser, the light of the longitudinal Zeeman effect is investigated. If the optical axis of the *λ*/4-plate coincides with the vertical, it is observed that some rings disappear if the analyser is at an angle of +45° with the vertical while other rings disappear for a position of –45°. That means that the light of the longitudinal Zeeman effect is polarized in a circular (opposed way). The *π*-lines are longitudinally not observable.

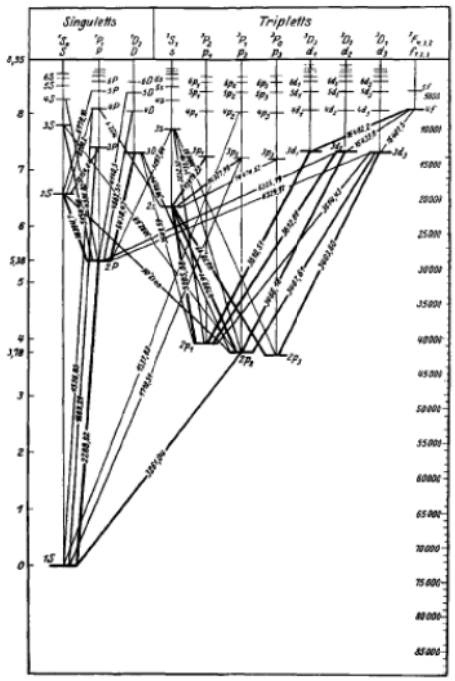

Fig. 4: The atomic state of Cadmium, wavelength in Å = 0.1 nm.

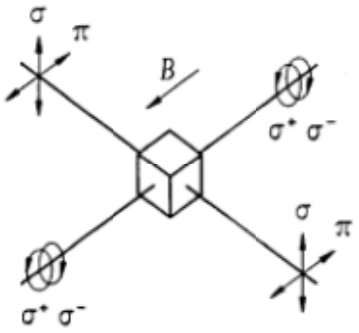

Fig. 5: Longitudinal and transversal Zeeman effect.

In the **normal Zeeman effect** with the transition 3 $^1D_2 \rightarrow 2\ ^1P_1$ with 643.847 nm the electron spins cancel each other in both the initial and final state and the energy of an atomic state in a magnetic field depends only on the magnetic moments of the electron orbit.
The magnetic moment of the orbital angular momentum is

$$\overrightarrow{\mu^1} = -\frac{e}{2m_e} \cdot \vec{l} = -g_l \mu_B \cdot \frac{\vec{l}}{\hbar}$$

with Bohr's magneton

$$\mu_B = \frac{e\hbar}{2m_e} = 9.274 \cdot 10^{-24} Am^2$$

and the gyromagnetic factor of orbital angular momentum $g_l = 1$.
In the vector model of the atom the energy shifts can be calculated. It is assumed, that angular moments and magnetic moments can be handled as vectors. Angular moment and the magnetic moment connected with it are antiparallel because of the negative electron charge. The amount of the orbital magnetic moment of the orbital angular momentum , with quantum number *l* such that

$$\left|\vec{l}\right| = \hbar\sqrt{l(l+1)}$$

, is:

$$\mu_1 = \mu_B\sqrt{l(l+1)}$$

In case of LS-coupling (Russel-Saunders coupling, spin-orbit coupling) for many electron systems is the amount of the total angular momentum

$$\left|\vec{J}\right| = \left|\vec{L} + \vec{S}\right| = \hbar\sqrt{J(J+1)}$$

with

$$\vec{S} = \sum \vec{s_i}$$

the sum of the spins of the single electrons and

$$\vec{L} = \sum \vec{l_i}$$

the sum of the orbit angular moments of the single electrons.
Here it is

$$\vec{S} = 0$$

So

$$\left|\vec{J}\right| = \left|\vec{L}\right| = \hbar\sqrt{L(L+1)}$$

The amount of the component of the corresponding magnetic moment $\overrightarrow{\mu_J}$ in direction of $\vec{J}$ is:

$$\left|\left(\overrightarrow{\mu_J}\right)_J\right| = |\overrightarrow{\mu_L}| = \mu_B\sqrt{L(L+1)} = g_J\mu_b\sqrt{J(J+1)}$$

with $g_J = 1$.
Observable is only the projection of the magnetic moment on $\vec{J}$

$$\left(\overrightarrow{\mu_J}\right)_J = -g_J\mu_J \cdot \frac{\vec{J}}{\hbar}$$

with it's quantization with respect to z-axis

$$(\overrightarrow{\mu_J})_{J,z} = -m_j g_J \mu_B$$

with the magnetic quantization number m_J with m_J = *J*, *J-1, …,-J*
The interaction energy with the outer magnetic field B_0 along the z-axis is then

$$V_{m_J} = -m_J g_J \mu_B B_0$$

Here the used transition for the **normal Zeeman effect** is 3 $D_2 \rightarrow 2\ ^1P_1$.

So in the initial state is *L = 2, S = 0* and *J = 2*. m_J may have the values m_J = -2, -1, 0, 1, 2. The gyromagnetic factor is g_i = 1 and the energy difference between two neighbouring substates of the initial state is then $\Delta E = -1\mu_B B_0$.
In the final state is *L = 1, S = 0* and *J = 1*. m_J may have the values m_J = -1, 0, 1. The gyromagnetic factor is g_f = 1 and the energy difference between two neighbouring sub-states of the final state is then$\Delta E = -1\mu_B B_0$, too, i.e. for transitions with the same Δm_J between initial and final state the energy shift is for initial and final state the same – so they have altogether the same frequency.
Fig. 6 shows the resulting transition diagram.
For electrical dipole transitions the selection rule states Δm_J = 1, 0, -1.
The energy shift of a transition between initial state with m_{Ji} and g_{Ji} and final state with m_{Jf} and g_f is then

$$V_{m_{J_i}} - V_{m_{J_f}} = \left(m_{J_f} g_f - m_{J_i} g_i\right) \mu_B B_0$$

and here the (m_{Jf} g_f – m_{Ji} g_i)-values are simply equal to Δm_J. So in case of LS-coupling in the normal Zeeman effect three equidistant lines are expected in this transition with a distance in frequency or wave number proportional to the magnetic field strength. The polarization of the transitions with Δm_J = 0 in transversal observation is parallel to the magnetic field (here horizontal) and of the other transitions the polarization is perpendicular to that.

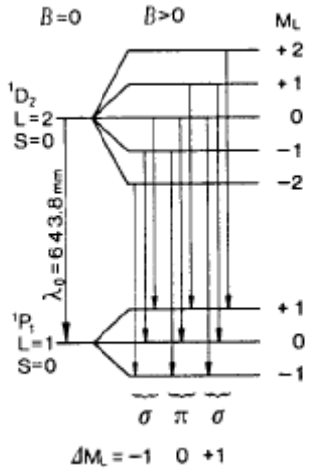

Fig. 6: Energy shift of the atomic states.

The **anomalous Zeeman effect** is the more general case where the electron spins do not cancel each other and the energy of an atomic state in a magnetic field depends on both the magnetic moments of electron orbit and electron spin.
The magnetic moment of the orbital angular momentum $\vec{l}$ is as above (see (*)) and the magnetic moment of the spin $\vec{s}$ is

$$\overrightarrow{\mu_s} = -\frac{e}{2m_e}\vec{s} = -g_s \mu_B \frac{\vec{s}}{\hbar}$$

with the gyromagnetic factor of orbital angular momentum g_s = 2.0023.
Additional to the orbital magnetic moment of the orbital angular momentum $\vec{l}$ the amount of the spin magnetic moment of the spin $\vec{s}$, with quantum number *s* such that

$$|\vec{s}| = \hbar\sqrt{s(s+1)}$$

has to be taken into account:

$$\mu_B = \left|-g_s \mu_B \sqrt{s(s+1)}\right|$$

In case of LS-coupling (Russel-Saunders coupling, spin-orbit coupling) for many electron systems the amount of the total angular momentum is

$$\left|\vec{J}\right| = \left|\vec{L} + \vec{S}\right| = \hbar\sqrt{J(J+1)}$$

with

$$\vec{S} = \sum \overrightarrow{s_\iota}$$

the sum of the spins of the single electrons and

$$\vec{L} = \sum \vec{l_\iota}$$

the sum of the orbit angular moments of the single electrons. In the vector model it is assumed, that angular moments and both spin and orbital magnetic moments can be handled as vectors. So the cosine rule applies for the sum of two vectors with an angle between them. The amount of the component of the corresponding magnetic moment $\overrightarrow{\mu_J}$ in direction of $\vec{J}$ is with the approximation $g_s \approx 2$:

$$\left|\left(\overrightarrow{\mu_J}\right)_J\right| = |\overrightarrow{\mu_L}|\cos\left(\vec{L},\vec{J}\right) + |\overrightarrow{\mu_s}|\cos\left(\vec{S},\vec{J}\right) = \mu_B\left(\sqrt{L(L+1)}\cos\left(\vec{L},\vec{J}\right) + 2\sqrt{S(S+1)}\cos\left(\vec{S},\vec{J}\right)\right)$$

$$\left|\left(\overrightarrow{\mu_J}\right)_J\right| = \frac{3J(J+1) + S(S+1) - L(L+1)}{2\sqrt{J(J+1)}}\mu_B = g_J\mu_B\sqrt{J(J+1)}$$

with

$$g_1 = 1 + \frac{J(J+1) + S(S+1) - L(L+1)}{2j(J+1)}$$

Observable is only the projection of the magnetic moment on $\vec{J}$

$$\left(\overrightarrow{\mu_J}\right)_J = -g_J\mu_B\frac{\vec{J}}{\hbar}$$

with it's quantization with respect to z-axis

$$\left(\overrightarrow{\mu_J}\right)_{J,z} = -m_J g_J \mu_B$$

with the magnetic quantization number m_J with $m_J = J, J-1, \ldots, -J$
The interaction energy with the outer magnetic field B_0 along the z-axis is then

$$V_{m_J} = -m_J g_J \mu_B B_0$$

Here for the **anomalous Zeeman effect** the used transition is is $2\,^3S_1 \rightarrow 2\,^3P_2$.

So in the initial state is L = 0, S = 1/2 + 1/2 = 1 and J = 1 + 0 = 1. m_J may have the values m_J = -1, 0, 1. The gyromagnetic factor is

$$g_i = 1 + \frac{1(1+1) + (1+1) - 0(0+1)}{2 \cdot 1(1+1)} 2$$

and the energy difference between neighbouring sub-states of the initial state is then

$$\Delta E = -2\mu_B B_0$$

In the final state is L = 1, S = 1 and J = 2. m_J may have the values m_J = -2, -1, 0, 1, 2. The gyromagnetic factor is

$$g_f = 1 + \frac{2(2+1) + (1+1) - 1(1+1)}{2 \cdot 2(2+1)} = \frac{3}{2}$$

and the energy difference between neighboured sub-states of the final state is then

$$\Delta E = -\frac{3}{2}\mu_B B_0$$

Fig. 7 shows the resulting transition diagram.

For electrical dipole transitions the selection rule states Δm_J = 1, 0, -1. The energy shift of a transition between initial state with m_{Ji} and g_{Ji} and final state with m_{Jf} and g_f is then

$$V_{m_{J_i}} - V_{m_{J_f}} = \left(m_{J_f} g_f - m_{J_i} g_i\right) \mu_B B_0$$

The following table shows the energy shifts of the transitions:

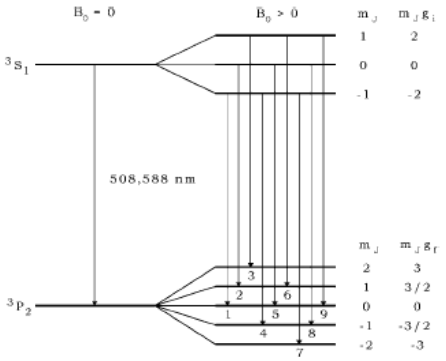

Fig. 7: Energy shift of the atomic states.

So in case of LS-coupling in the anomalous Zeeman effect nine equidistant lines are expected in this transition instead of three without spin magnetism. The polarization of the transitions with Δm_J = 0 in transversal observation is parallel to the magnetic field (here horizontal) and the polarization of the other transitions is perpendicular to the magnetic field.

At observing the σ-lines of the transversal Zeeman effect it is easy to see that the amount of splitting increases with increasing magnetic field strength. For a quantitative measurement of this splitting in terms of number of wavelengths, a Fabry-Perot interferometer is used, the functioning of which has to be explained:

The Fabry-Perot étalon has a resolution of approximately 400000. That means that a wavelength change of less then 0.002 nm can still be detected.

The étalon consists of a quartz glass plate of 3 mm thickness coated on both sides with a partially reflecting layer (90 % reflection, 10 % transmission). Let us consider the two partially transmitting surfaces (1) and (2) in Fig.8 seperated by a distance t. An incoming ray forming an angle with the plate normal will be split into the rays AB, CD, EF, etc. the path difference between the wave fronts of two adjacent rays (e.g. AB and CD) is

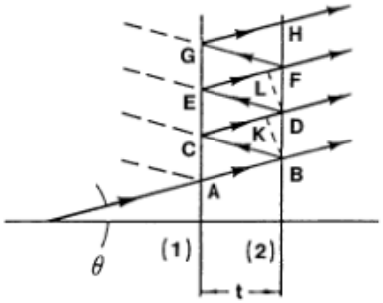

Fig. 8: Reflected and transmitted rays at the parallel surfaces (1) and (2) of the étalon. The étalon spacing is t = 3 mm.

$$\delta = \mu \cdot (BC + CK)$$

where BK is defined normal to CD and μ is the refractive index of quartz at 509 nm, μ = 1.4519. At 644 nm is μ = 1.4560. With

$$CK = BC \cos 2\theta$$

and

$$BC \cdot \cos\theta = t$$

we obtain

$$\delta = \mu \cdot BCK = \mu \cdot BC(1 + \cos 2\theta) = 2\mu \cdot BC \cos^2\theta = 2\mu \cdot t \cdot \cos\theta$$

and for a constructive interference it is:

$$n\lambda = 2\mu \cdot t \cdot \cos\theta \qquad (1)$$

where n is an integer and l the light's wavelength. Equation (1) is the basic interferometer equation. Let the parallel rays B, D, F, etc. be brought to a focus by the use of a lens of focal length f as shown in Fig. 9.

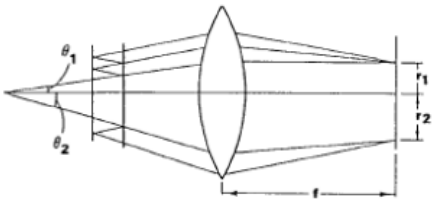

Fig. 9: Focusing of the light emerging from a Fabry-Perot étalon. Light entering the étalon at an angle θ is focused onto a ring of radius $r = f\theta$ where f is the focal length of the lens.

For θ fulfilling equation (1) bright rings will appear in the focal plane with the radius

$$r_n = f \tan\theta_n \approx f\theta_n$$

for small values θ_n, e.g. rays nearly parallel to the optical axis.
Since

$$n = \frac{2\mu \cdot t}{\lambda}\cos\theta_n = n_0 \cos\theta_0 = n_0\left(1 - 2sin^2\frac{\theta_n}{2}\right)$$

with

$$n_0 = \frac{2\mu \cdot t}{\lambda}$$

we finally obtain

$$n = n_0\left(1 - \frac{\theta_n^2}{2}\right)$$

or

$$\theta_n = \sqrt{\frac{2(n_0 - n)}{n_0}} \qquad (3)$$

If θ_n corresponds to a bright fringe, n is an integer. However is n_0 the interference condition for the center (for θ = 0) generally not an integer.
If n_1 is the interference order of the first ring, it is $n_1 < n_0$ since $n_1 = n_0 \cos\theta_n$. We then let

$$n_1 = n_0 - \varepsilon; 0 < \varepsilon < 1$$

where n_1 is the closest integer to n_0 (smaller than n_0). In general is for the p^{th} ring of the pattern, measured starting from the center, the following is valid:

$$n_p = (n_0 - \varepsilon) - (n_p - 1) \quad (4)$$

Combining equation (4) with equations (2) and (3), we obtain for the radii of the rings, writing r_p for r_{n_p},

$$r_p = \sqrt{\frac{2f^2}{n_0}} \cdot \sqrt{(p-1) + \varepsilon} \quad (5)$$

We note that the difference between the squares of the radii of adjacent rings is a constant:

$$r_{p+1}^2 - r_p^2 = \frac{2f^2}{n_0} \quad (6)$$

ε can be determined graphically plotting r_p^2 versus p and extrapolating to $r_p^2 = 0$.
Now, if there are two components of a spectral line (splitting of one central line into two components) with wavelengths λ_a and λ_b, which are very close to one another, they will have fractional orders at the center ε_a and ε_b:

$$\varepsilon_a = \frac{2\mu \cdot t}{\lambda_a} = -n_{1,a} = 2\mu \cdot t \cdot k_a - n_{1,a}$$

$$\varepsilon_b = \frac{2\mu \cdot t}{\lambda_b} = -n_{1,b} = 2\mu \cdot t \cdot k_b - n_{1,b}$$

where k_a and k_b are the corresponding wave numbers and $n_{1,a}$, $n_{1,b}$ is the interference order of the first ring. Hence, if the rings do not overlap by a whole order so $n_{1,a} = n_{1,b}$ and the difference in wave numbers between the two components is

$$\Delta k = k_a - k_b = \frac{\varepsilon_a - \varepsilon_b}{2\mu \cdot t} \quad (7)$$

Using equations (5) and (6), we get

$$\frac{r_{p+1,a}^2}{r_{p+1}^2 - r_p^2} - p = \varepsilon \quad (8)$$

Applying equation (8) to the components *a* and *b*, yields

$$\frac{r_{p+1,a}^2}{r_{p+1,a}^2 - r_{p,a}^2} - p = \varepsilon_a$$

and

$$\frac{r_{p+1,b}^2}{r_{p+1,b}^2 - r_{p,b}^2} - p = \varepsilon_b$$

By substituting these fractional orders into equation (7), we get for the difference of the wave numbers:

$$\Delta k = \frac{1}{2\mu \cdot t}\left(\frac{r_{p+1,a}^2}{r_{p+1,b}^2 - r_p^2} - \frac{r_{p+1,b}^2}{r_{p+1,b}^2 - r_{p,b}^2}\right) \quad (9)$$

From equation (6) we get the difference between the squares of the radii of component *a*:

$$\Delta_a^{p+1,p} = r_{p+1,a}^2 - r_{p,a}^2 = \frac{2f^2}{n_{0,a}}$$

this is equal to (within a very small part) the same difference for component *b*

$$\Delta_b^{p+1,p} = r_{p+1,b}^2 - r_{p,b}^2 = \frac{2f^2}{n_{0,b}}$$

Hence we assume

$$\Delta_a^{p+1,p} = \Delta_b^{p+1,p}$$

for all values of *p*. Similarly, all values

$$\delta_{a,b}^p = r_{p+1,a}^2 - r_{p+1,b}^2$$

must be equal, regardless of *p* (the order of interference) and their average may be taken as may be done for the different *Δ*-values. With *δ* (the difference of squares of radii of different lines of the same order of interference) and *Δ* (difference of squares of radii of different orders) as average values we get for the difference of the wave numbers of the components *a* and *b*:

$$\Delta k = \frac{1}{2\mu \cdot t} \cdot \frac{\delta}{\Delta} \quad (10)$$

Note: Equation (10) shows that *Δk* does not depend on the dimensions used in measuring the radii of the ring system.

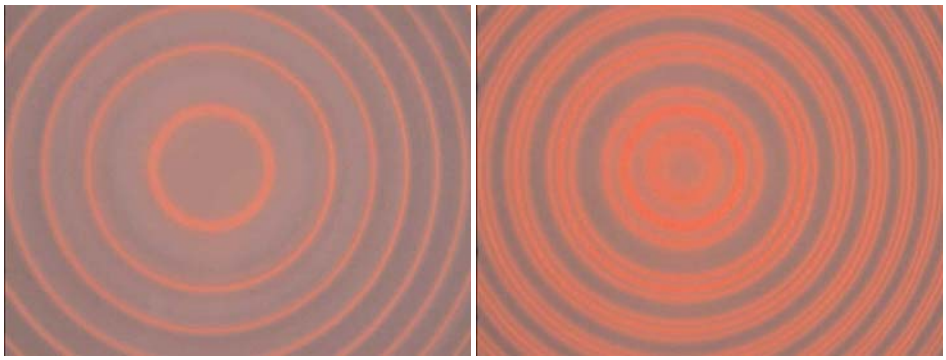

Fig. 10: Normal Zeeman effect: Interference pattern without polarisation filter for no coil current and for 5 A coil current. On the left there is one ring per order of interference, on the right there are three rings per order of interference.

Anomalous Zeeman effect: For all these pictures the coil current was set such that the different orders of interference were just still separated. This was the case with 5 A on the magnet coils. In Fig. 11 all the rings are visible but hard to count. In Fig. 12 the middle three rings are visible with $\Delta m_j = 0$. In Fig. 13 the outer and inner three rings with $\Delta m_j = \pm 1$ are visible, that's six rings making a total of nine rings. The rings seem to be equidistant but not of the same intensity.

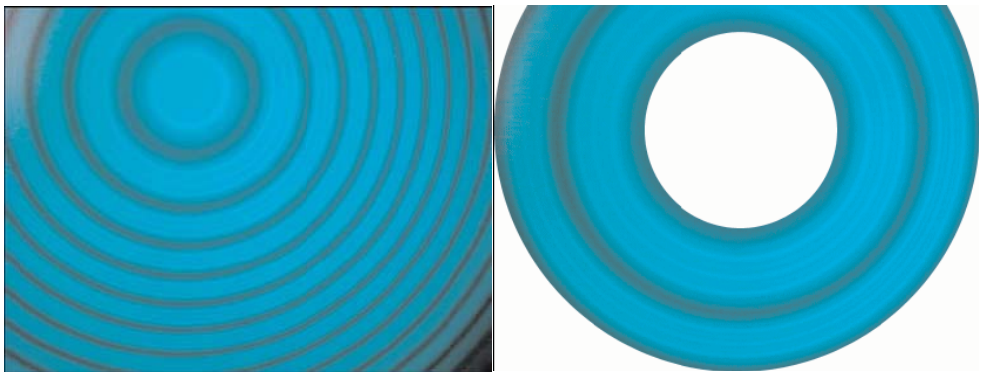

Fig. 11: Anomalous Zeeman effect: Interference pattern without polarisation filter and magnified cut-out of the first completely visible two orders of interference.

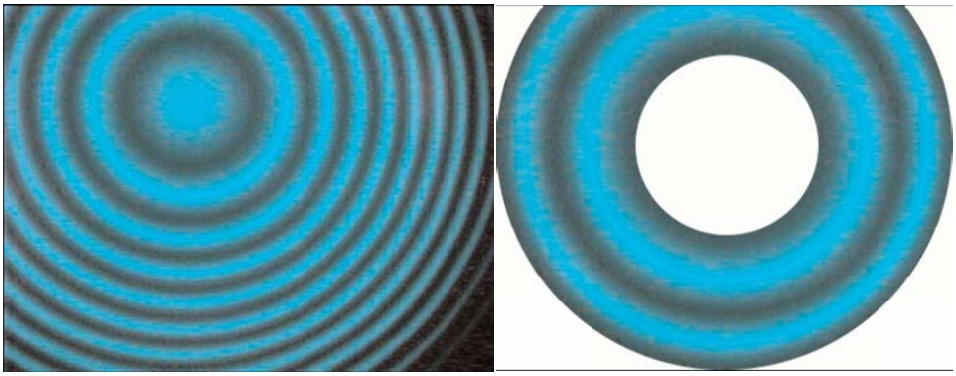

Fig. 12: Anomalous Zeeman effect: Interference pattern with horizontal polarisation filter and magnified cut-out of the first complete two orders.

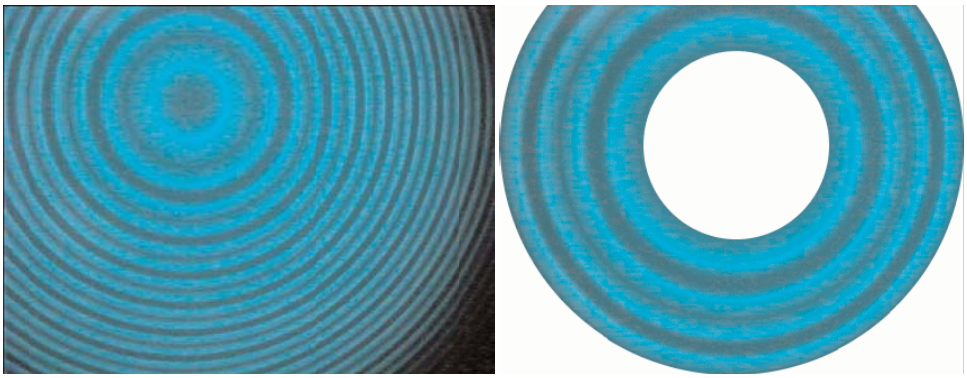

Fig. 13: Anomalous Zeeman effect: Interference pattern with vertical polarisation filter and magnified cut-out of the first complete two orders.

Measurement and Evaluation

The radii of the rings have to be measured at different magnetic flux densities. With equation (10) the corresponding difference in wave numbers Δk is then determined. We proceed in two steps: First we take pictures of the ring patterns at different coil currents/magnetic field strengths. Then in a second step the ring diameters in these pictures are measured.

To get a life picture from the camera go to the <File> menu and choose the entry <Capture Window>. In the capture window the settings regarding e.g. contrast, brightness and saturation of the image can be optimised via the menu you get to when choosing <Video Capture Filter> from the <Option> menu.
When satisfied with the image quality and a certain coil current (magnetic field) is established, the picture is captured by choosing <Still Image> from the <Capture> menu. At this stage it is advisable to go to the main window and write the value of the coil current and the polarization at which the picture was taken into it by using the <Text> tool. This prevents a mix-up later on.

Normal Zeeman effect:
The above procedure is repeated using different magnetic fields without polarization filter in transversal observation for coil currents such that the observed ring patterns of different orders do not overlap. Once these pictures have been collected, proceed to measure the radii of the rings choosing <Circle> from the <Measure> menu. By moving the mouse across the picture, a circle is drawn. Fit this circle in size and position as good as possible to a ring of interest. You will see that radius, area and perimeter of the circle will be displayed in a little box and in a table below the picture (cf. Fig.14). What we are mainly interested in is the square of the radius of the circle – so we can use the area data. Note that the units (µm, mm, cm) are of no importance in this experiment, that means no calibration of the camera has to be performed and the factor π = 3.14159 … can be neglected.

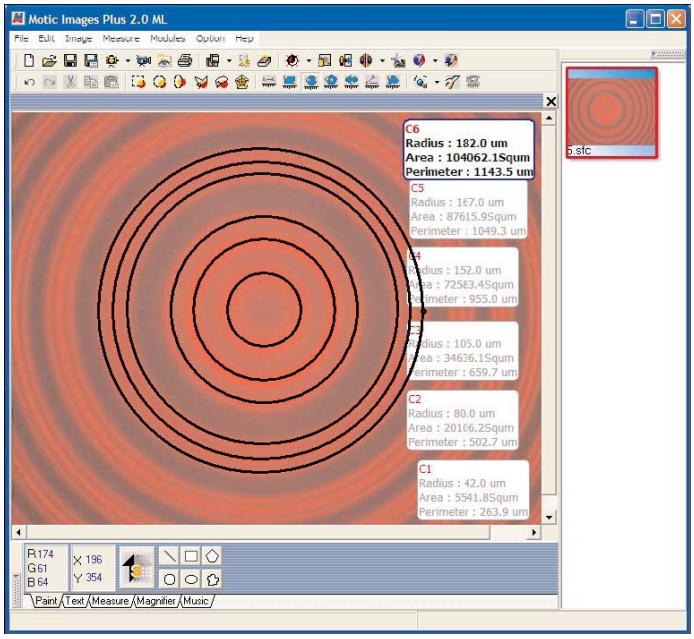

Fig. 14: Screenshot of software used to measure the radii of interference rings, evaluation of horizontal and vertical polarisation.

All the visible rings may be evaluated, i.e. three rings per order of interference, the middle one of them with unchanged wavelength. Proceed to draw and fit circles to as many orders of rings as are suitable in the picture, this will give you $r_{1,a}$, $r_{1,b}$ $r_{1,c}$; $r_{2,a}$, $r_{2,b}$ $r_{2,c}$; $r_{3,a}$, $r_{3,b}$ $r_{3,c}$; … . Do the same with the other pictures captured. In the classical version without the CCD-camera for each field strength a set of radii of rings is determined in the following way: The slash of the scale „0“ is shifted horizontally along a diameter through the ring pattern until it coincides e.g. with the outer ring of the fourth order to the left into which the fourth ring has split. Always approach from the same side, e.g. from left to right, for correct readings. The first value is denoted. The „0“ slash is then moved from left to right, the next reading taken at the middle ring of the 4th ring system, the next at the inner ring of the 4th ring system and so on until the outer ring on the right of the 4th ring system is reached. The last reading minus the first reading divided by two then provides the radius $r_{4,c}$ and so on. Using the slide mount, all readings are done in “mm“ with a precision of 1/100th of a mm.
In Fig.15 for a given field strength d was calculated from the differences of areas of corresponding rings of different order number and subsequent averaging (e.g. difference of area between middle ring of second order and middle ring of first order) and *d* was calculated from the differences of ring areas of the three rings of the same order number (outer to middle and middle to inner) and subsequent averaging over all values.

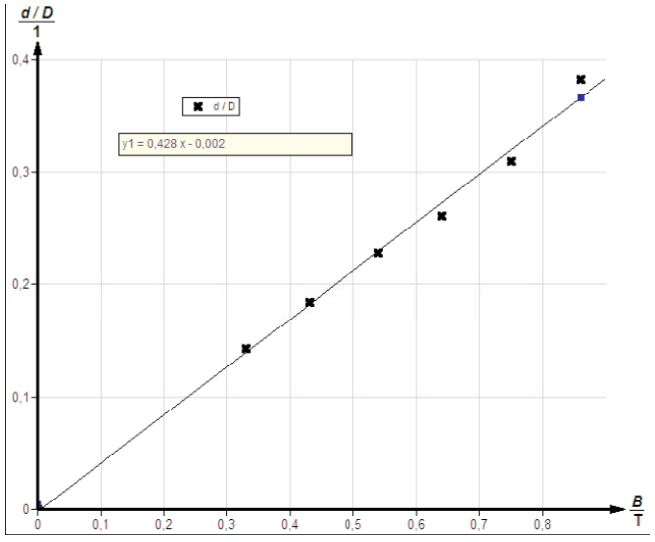

Fig. 15: Measurement results for δ vs. magnetic field strength.

With

$$\Delta V = \mu_B B_0 = hc\Delta k = \frac{hc}{2\mu \cdot t} \cdot \frac{\delta}{\Delta}$$

so

$$\mu_B = \frac{hc}{2\mu \cdot t \cdot B_0} \cdot \frac{\delta}{\Delta}$$

With

$$\frac{\delta}{\Delta B_0} = 0.428 \frac{1}{T}$$

from the regression of the measured values and μ = 1.456, h = 6.63 · 10^{-34} Js, c = 2.99 · 10^{8} m/s, this yields

$$\mu_B = 9.71 \cdot 10^{-24} \frac{J}{T}$$

The literature value is $\mu_B = 9.273 \cdot 10^{-24} \frac{J}{T}$.

Anomalous Zeeman effect:
The above procedure is repeated without the red colour filter and now using the green interference filter. Capture pictures for different coil current strengths for each horizontal and vertical polarization in transversal observation for coil currents such that the observed ring patterns of different orders do not overlap so much, that the rings of interest can no longer be distinguished, i.e less than 7.5 A for vertical and less than 12 A for horizontal polarization. High currents may not be sent through the coils for a long time since they might heat up!
Once these pictures have been taken, proceed to measure the radii of the rings choosing <Circle> from the <Measure> menu.
For horizontal polarization the three visible inner rings per order may be evaluated. For vertical polarization the inner two rings of the set of six rings per order may be evaluated since they are the best visible ones – the other rings are not well separated. Proceed to draw and fit circles to as many orders of rings as are suitable in the picture, this will give you squares of $r_{1,a}$, $r_{1,b}$; $r_{2,a}$, $r_{2,b}$; $r_{3,a}$, $r_{3,b}$; … . Do the same with the other pictures captured.
In Fig. 16 in the horizontal polarization the sizes of the rings of the lines with number 3 and 6 according to Fig. 7 were evaluated. Their energy difference is

$$\Delta V = 2\mu_B B_0 = hc\Delta k = \frac{hc}{2\mu \cdot t} \cdot \frac{\delta}{\Delta}$$

so

$$\mu_B = \frac{hc}{4\mu \cdot t \cdot B_0} \cdot \frac{\delta}{\Delta}$$

with

$$\frac{\delta}{\Delta B_0} = 0.892 \frac{1}{T}$$

from the regression of the measured values and μ = 1.452, h = 6.63 · 10^{-34} Js, c = 2.99 · 10^{8} m/s, this yields

$$\mu_B = 10.1 \cdot 10^{-24} \frac{J}{T}$$

In Fig. 17 in the vertical polarization the sizes of the rings of the lines with number 4, 5, 6 according to

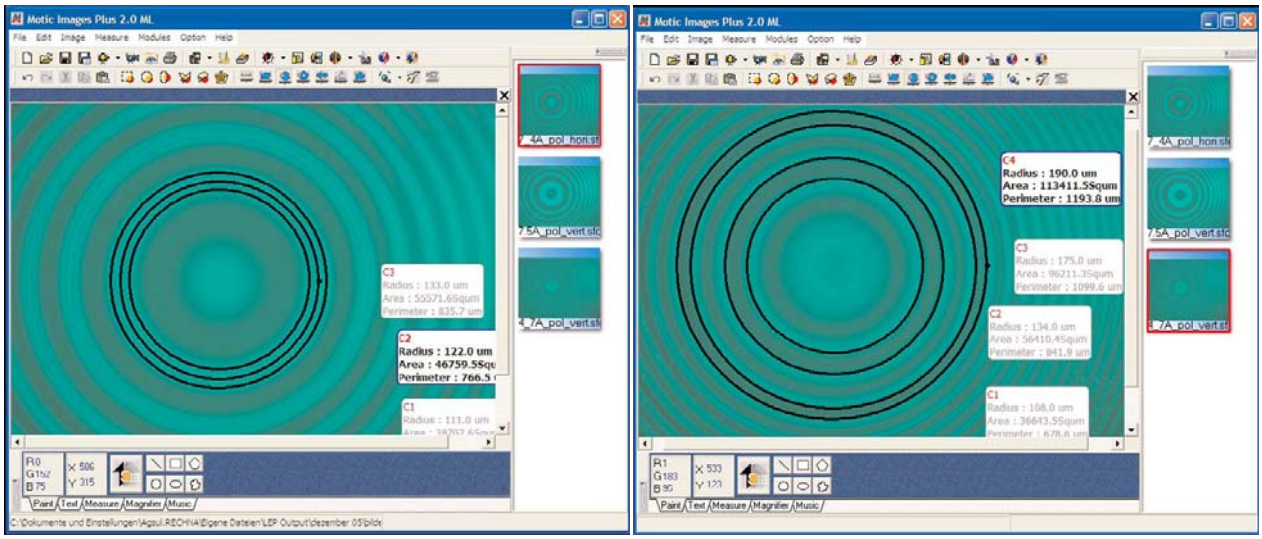

Fig. 16: Screenshot of software used to measure the radii of interference rings, evaluation of horizontal and vertical polarisation.

Fig. 7 were evaluated. Their energy difference is

$$\Delta V = \frac{1}{2}\mu_B B_0 = hc\Delta k = \frac{hc}{2\mu \cdot t} \cdot \frac{\delta}{\Delta}$$

so

$$\mu_B = \frac{hc}{\mu \cdot t \cdot B_0} \cdot \frac{\delta}{\Delta}$$

with

$$\frac{\delta}{\Delta B_0} = 0.172 \frac{1}{T}$$

from the regression of the measured values and μ = 1.452, h = 6.63 · 10^{-34} Js, c = 2.99 · 10^{8} m/s, this yields

$$\mu_B = 7.82 \cdot 10^{-24} \frac{J}{T}$$

The average of both is $\mu_B = 8.96 \cdot 10^{-24} \frac{\mathrm{J}}{\mathrm{T}}$.

The literature value is $\mu_B = 9.273 \cdot 10^{-24} \frac{J}{T}$.

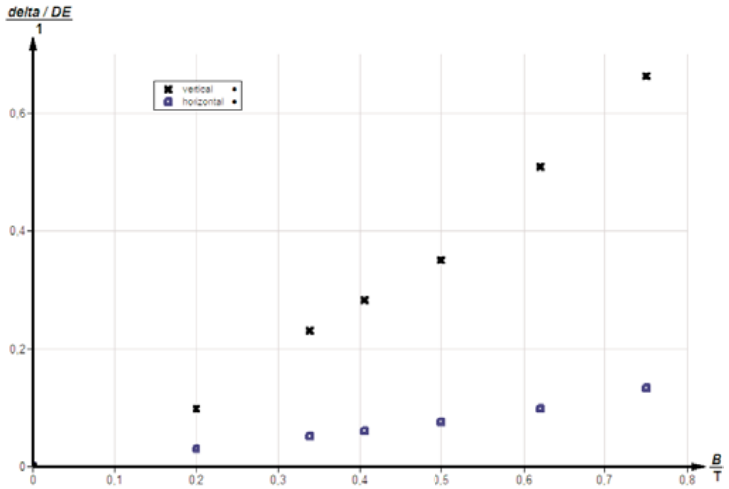

Fig. 17: Measurement results for δ/Δ vs. magnetic field strength.